INT. J. NUM. METH. HEAT FLUID FLOW, VOL. 6, NO. 7, 31–46 (1996)

A NUMERICAL STUDY OF NATURAL CONVECTION IN A VERTICAL ANNULUS WITH CONSTANT HEAT FLUX ON THE INNER WALL

J.G.WEI AND W.Q. TAO

School of Energy and Power Engineering, Xi'an Jiaotong University, Xi'an Shaanxi 710049, China

ABSTRACT

A numerical study of natural convection of air in a vertical annulus has been conducted, where the inner wall is heated with constant heat flux at its inner side, the outer wall of the annulus being maintained at constant temperature, and the top and bottom plates are assumed to be insulated. The cases of radius ratio $K = 3$, aspect ratio $A = 10\sim30$, and $Ra^* = 10^3\sim1.7 \times 10^7$ have been simulated. Both axial conduction and surface radiation are taken into account to reveal their effects on the distributions of inner wall temperature and local Nusselt number. Emphasis is on the comparison between the numerical results and the relevant experimental data, and the comparison between numerical solutions with and without considering the surface radiation. The numerical results of heat transfer are found to be in good agreement with the corresponding experimental results in the literature. The dependence of average relative conductivity on aspect ratio and the effect of imperfection in top and bottom insulation on the inner wall temperature are also discussed.

KEY WORDS Natural convection Vertical annulus Numerical study Constant heat flux

NOMENCLATURE

a	= Thermal diffusivity
$a_{E,W,N,S}$, a_P	= Coefficients in discretization equation
A	= Aspect ratio L/δ
g	= Gravitational acceleration
J	= Radiosity
k	= Thermal conductivity
K	= Radius ratio r_0/r_i
K_{eq}	= Average relative conductivity
K_{sf}	= Conductivity ratio of solid to liquid K_s/K_f
L	= Length of annulus
$L1$	= Grid number in x direction
$M1$	= Grid number in r direction
N	= Number of radiative surfaces divided
Nu	= Local Nusselt number
P	= Dimensionless pressure
Pr	= Prandtl number ν/a
q	= Heat flux
r	= Radial co-ordinate
R	= Dimensionless radial co-ordinate r/δ
Ra^*	= Modified Rayleigh number $\beta g(q\delta/k_f)\delta^3/(a\nu)$
T	= Dimensionless temperature $(T' - T_0')/(q\delta/k_f)$
T'	= Dimensional temperature
T_m	= Dimensionless average temperature on the inner wall
u	= Velocity in x direction
U	= Dimensionless velocity in x direction $u\delta/\nu$
v	= Velocity in r direction
V	= Dimensionless velocity in r direction $v\delta/\nu$
x	= Vertical co-ordinate
X	= Dimensionless vertical co-ordinate x/δ
X_{ij}	= View factor of ith to jth radiative surface
β	= Thermal expansion coefficient
Γ	= Nominal diffusion coefficient
δ	= Gap width $r_0 - r_i - w$
ΔT	= Mean temperature difference between inner and outer wall
ε	= Emissivity
ν	= Kinematic viscosity
σ	= Stefan-Boltzmann constant

Subscripts

e	= Eastern interface
f	= Fluid
i	= Inner wall
o	= Outer wall
r	= Radiation
s	= Solid

0961–5539

Received June 1995
Revised October 1995

INTRODUCTION

This paper presents results of a numerical study of natural convection in a vertical annulus where the inner wall is of finite thickness and heated with constant heat flux at its inner side, the outer wall of the annulus being at constant temperature and the top and bottom plates are adiabatic. Natural convection heat transfer in a vertical annulus is an important method of energy transfer and numerous applications are found in different engineering fields such as energy conversion, storage and transmission systems. Examples of using the natural convection in vertical annulus include the heat transfer from a nuclear reactor fuel rod bundle to the interior of its canister and the cooling of isolated phase buses in power plants. Many experimental and/or numerical investigations on this problem have been performed in the past. Only those which are closely related to the present study are briefly reviewed here. The thermal boundary conditions in the works conducted by Sheriff[1], Keyhani *et al.*[2], Bhushan *et al.*[3], Shang *et al.*[4] and Khan and Kumar[5] are of the same type as the present study. For this type of thermal boundary condition, accurate subtraction of the radiation heat transfer rate in the enclosure from the total power input at the inner side is crucial in the test data reduction. When numerical method is used, the radiative heat transfer between inner and outer surfaces must be taken into account since the surface temperature of the inner wall cannot be specified *a priori*. Sheriff[1] conducted experiments with CO_2-filled vertical annuli of radius ratios $K = 1.03$, 1.11, and 1.23 for aspect ratio $A = 38$, 76, and 228 with Rayleigh numbers ranging from 10^5 to 10^8. In order to correct for the thermal radiation, he performed some preliminary experiments at low pressure to ensure that the heat transferred was only by conduction and radiation. By subtraction of the axial and radial heat conduction, he obtained the thermal radiant heat transfer rate. Keyhani *et al.*[2] performed experiments with air and helium as test fluid for $K = 4.33$ and $A = 27.6$ for a range of Rayleigh numbers from 10^3 to 2.3×10^6. It is reported that energy transferred by the thermal radiation varies according to Rayleigh number, and working fluid. For air, radiation can account for up to 50 per cent, and for helium, 30 per cent of the total heat transfer. The temperature distribution on the heated wall presented by Keyhani *et al.*[2] shows that, at a high Rayleigh number, the inner wall temperature distribution is quite uneven; it increases from the bottom to the midsection and then decreases significantly from midsection to the top. In their Rayleigh number range studied, the maximum local wall temperature difference may be as large as 50°C. Bhushan *et al.*[3] extended the work of Keyhani *et al.*[2] for two other combinations of aspect and diameter ratio, $A = 52.82$, $K = 2.77$ and $A = 38.38$, $K = 8.28$. The temperature distribution along the heated inner wall has the same pattern as observed in Keyhani *et al.*[2] with a better smoothness. Shang *et al.*[4] obtained temperature data and heat transfer results experimentally using air for $K = 3$, $A = 22.5$ and $10^3 \leq Ra^* \leq 1.7 \times 10^7$. Their temperature distribution data on the inner surface exhibit rather a flat character, with a maximum difference from the bottom to the top of about 10°C. Khan and Kumar[5] obtained numerical results for $1 \leq K \leq 15$, $1 \leq A \leq 10$ and $100 < Ra^* < 10^7$ by solving the Navier-Stokes equations with the vorticity-stream function method. They found that the inner wall temperature distribution was dependent on the diameter ratio and the aspect ratio. The numerically predicted wall temperature distributions were characterized by the smooth increase of wall temperature from the bottom to the top. It should be noted that, in their computation, the radiative heat transfer between the inner surface and the outer one was not taken into account.

From the above brief review of the literature, it can be seen that the investigations, especially the numerical ones, pertinent to the above boundary conditions, are rather limited. In addition, there are two kinds of temperature profile on the inner wall observed in the experiments or predicted by the numerical method. One was obtained by Keyhani *et al.*[2] and Bhushan *et al.*[3] Their results are characterized by the existence of a higher temperature region in the midsection of the annulus and two rapid decrease regions towards the two ends of the annulus. The results obtained by Shang *et al.*[4] and Khan and Kumar[5] are of the other type, which shows a smooth and almost monotonic increase in wall temperature from the bottom to the top for high Rayleigh number cases. However, the variation of inner wall temperature from the bottom to top obtained by Khan

and Kumar[5] seems to be more significant than that observed in the experiments of Shang *et al.*[4] In the numerical study of Khan and Kumar[5], the radiative heat transfer between the inner and outer surfaces was not considered, which, in the authors' expectation, may partly account for this difference.

Thus, in order to enhance our understanding of the effects of radiation on natural convection heat transfer in the annulus, especially on the temperature distribution along the inner wall, and to extend further the geometric parameters of numerical data, the present work deals with the numerical computations of natural convection in a vertical annulus with constant heat flux on the inner wall for $K = 3$ and $A = 22.5$, and $10^3 \leq Ra^* \leq 1.7 \times 10^7$. These parameters are copied from the experimental work conducted by Shang *et al.*[4], so that the numerical results can be compared with their experimental ones. Both axial conduction and radiation are taken into account in the calculations to reveal their effects on the inner wall temperature distribution. In addition, the aspect ratio is varied systematically from 10 to 30, and the dependence of average relative conductivity on aspect ratio is then evaluated.

PROBLEM FORMULATION

Consider an air-filled annular space bounded by two vertical concentric cylinders of radii r_i and r_o, with the inner cylinder having a thickness of w. As shown in *Figure 1*, the inner surface of the inner cylinder is maintained at constant heat flux and the outer cylinder of the annulus at constant temperature T_o. Assuming that the Boussinesq approximation is valid, the dimensionless equations governing the steady, axisymmetric laminar fluid flow with negligible viscous dissipation may be reduced to:

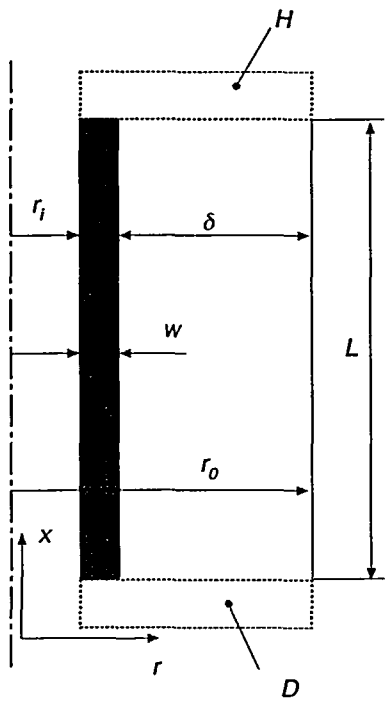

Figure 1 Schematic of computational domain

$$\frac{\partial U}{\partial X}+\frac{1}{R}\frac{\partial (RV)}{\partial R}=0 \tag{1}$$

$$U\frac{\partial U}{\partial X}+V\frac{\partial U}{\partial R}=-\frac{\partial P}{\partial X}+\Gamma\nabla^2 U+\frac{Ra^*}{Pr}T \tag{2}$$

$$U\frac{\partial V}{\partial X}+V\frac{\partial V}{\partial R}=-\frac{\partial P}{\partial R}+\Gamma\nabla\, V-\frac{V}{R^2} \tag{3}$$

$$U\frac{\partial T}{\partial X}+V\frac{\partial T}{\partial R}=\frac{K_r}{Pr}\nabla^2 T \tag{4}$$

The dimensionless quantities are defined as follows:

$$X=\frac{x}{\delta};\quad R=\frac{r}{\delta};\quad K_r=\frac{k_r}{k_f}$$

$$U=u\frac{\delta}{\nu};\quad V=v\frac{\delta}{\nu};\quad T=\frac{T'-T_c'}{\frac{q\delta}{k_f}}$$

$$Ra^*=\frac{\beta g(\frac{q\delta}{k_f})\delta^4}{a\nu};\quad K=\frac{r_o}{r_i};\quad A=\frac{L}{\delta} \tag{5}$$

The boundary conditions can be written as:

$$R=\frac{r_i}{\delta},\quad U=0;\ V=0;\quad \frac{\partial T}{\partial R}=-\frac{1}{K_r} \tag{6}$$

$$R=\frac{r_o}{\delta},\quad U=0;\ V=0;\ T=0 \tag{6b}$$

$$X=0,\quad U=0;\ V=0;\quad \frac{\partial T}{\partial X}=0 \tag{6c}$$

$$X=A,\quad U=0;\ V=0;\quad \frac{\partial T}{\partial X}=0 \tag{6d}$$

This set of boundary conditions was adopted for the computation domain shown by the solid line in *Figure 1*, where the top and bottom surfaces were assumed to be perfectly insulated. To examine the imperfection in top and bottom insulation, the computation domain was extended axially to the regions H and D confined by the dashed line. The thermal conductivity of these two extended regions was taken as 0.037W/m·°C, which was obtained from the direct measurement of the insulating materials used in the test of Shang *et al.*[4] The thicknesses of the H and D were 50mm and 40mm respectively, which were the same as Shang's work. For these extended regions, the surface temperatures at the top and bottom were assumed to be the same temperature as the cooling medium surrounding the annulus, which was also consistent with the condition in Shang's test, where a circulating cooling water was used to cool the outside surface of the test apparatus.

In order to take the thermal radiation into account, the annulus is regarded as a radiative network consisting of N isothermal surfaces. The equations concerning the radiation heat transfer are[6]:

$$q_r(i) = \frac{\varepsilon(i)}{1-\varepsilon(i)}[\sigma T^4(i) - J(i)], \quad i = 1,2,\ldots,N \tag{7}$$

$$J(i) = \sigma\varepsilon(i)T^4(i) + (1-\varepsilon(i))\sum_{j=1}^{N} J(j)X_{ij}, \quad i = 1,2,\ldots,N \tag{8}$$

The entire computation domain includes both fluid and solid regions. Thus, the present study is actually a coupled conduction and convection heat transfer problem with radiation on solid surfaces.

NUMERICAL METHOD

For the computational domain shown in *Figure 1*, the temperature fields in both solid and gas regions are obtained by solving equations (1)-(4) with appropriate values of K_{sf}, Γ, and Ra^* as given in *Table 1*. The number of radiative surfaces, N, in equation (7) and equation (8) is taken to be 16 in the present study.

The differential equations were discretized with the finite volume integration method. The convective-diffusive terms were approximated by the power-law scheme. The SIMPLEC algorithm was employed to deal with the linkage between pressure and velocity, and the resulting linear system of algebraic equations was solved by the SLUR method. More details may be found in the book by Tao[7]. The method proposed by Yang *et al.*[8] was used to treat the thermal radiation at the interface of solid and gas regions, i.e. the outer surface of the inner cylinder. In this method, the radiative heat flux at inner surfaces is treated as an additional source term for the control volumes neighbouring with the inner surfaces. It can be shown that for any control volume in the solution domain, the discretized energy equation can be written in the following form:

$$a_P\phi_P = a_E\phi_E + a_W\phi_W + a_N\phi_N + a_S\phi_S + S_{c,ad}\Delta x\Delta y$$

where the additional source term, $S_{c,ad}$, comes from the surface radiation heat flux and can be determined by the following equations.

For the air-side control volume (*Figure 2*)

$$S_{c,ad} = \frac{q_r\delta x^-/k_f}{\delta x^-/k_f + \delta x^+/k_\varepsilon}\cdot\frac{1}{\Delta x^+} \tag{9a}$$

and for the solid-side control volume

$$S_{c,ad} = \frac{q_r\delta x^+/k_\varepsilon}{\delta x^-/k_f + \delta x^+/k_\varepsilon}\cdot\frac{1}{\Delta x^-} \tag{9b}$$

The net radiative heat flux, q_r, at the solid-gas surface can be calculated from equation (7). The average interfacial temperature of surface i, $T(i)$, is interpolated from neighbouring grid points

Table 1 Values of K_{sf}, Γ, Ra^* and Pr in various regions

Region	K_{sf}	Γ	Ra^*	Pr
Fluid	1.0	1.0	As is	0.7
Tube wall	6,100.0	10^{30}	0	–
End insulation				
H and D	1.48	10^{30}	0	–

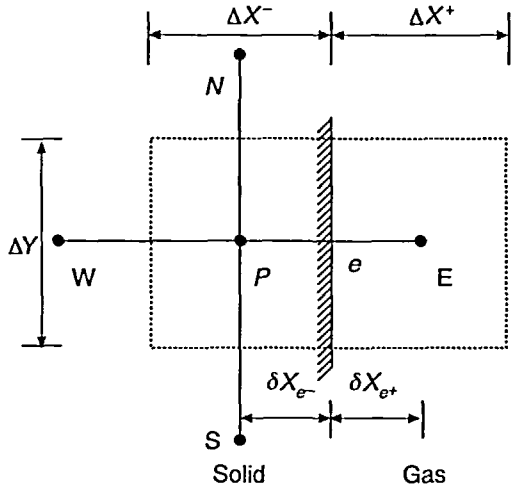

Figure 2 Solid-gas control volumes

according to the flux continuity condition. For example, the temperature of *e*-interface in *Figure 2* is

$$T_e = \frac{T_P k_P/\delta x_e + T_E k_E/\delta x_e^+ - q_r}{k_P/\delta x_e + k_E/\delta x_e^+} \tag{10}$$

Because of the strong nonlinearity of radiative heat transfer, the solution procedure is iterative in nature. To avoid divergence of iteration, the value of q_r should be under-relaxed. For details, Zhao and Tao[9] may be consulted.

Grid independence of results was checked and ensured. The problem of pure convection for air in the annulus without considering the axial conduction and surface radiation was used for this purpose. Several different sized grids were used in this work as part of grid independence investigation: $L1 \times M1 = 33 \times 32$, 53×42, 63×62, 103×102. The results of a grid independence investigation for $K = 3$, $A = 22.5$ and $Ra^* = 2 \times 10^7$ are given in *Table 2*. A mesh of 53×42 nodal points leads to a value of the average relative conductivity 1.2 per cent larger than that given by a mesh of 103×102. Furthermore, to reveal the effect of surface number of radiative exchange on the inner wall and local Nusselt number distributions, two preliminary cases were computed. In one case the total enclosure was divided into eight radiative surfaces while in the other 16 surfaces were divided. The differences in wall temperature and local Nusselt number were not appreciable, with a maximum deviation of 1.5 per cent. To keep the convergence time to a minimum without losing accuracy, a grid of 53×42 nodes and 16 radiative exchange surfaces were used for most cases investigated in the present study.

The following criterion was used for checking convergence at each point:

$$|\phi_{new} - \phi_{old}|/|\phi_{new}|_{\max} \leq \in$$

Table 2 Grid number test results

$L1 \times M1$	K_{eq}
33×32	5.233
53×42	5.197
63×62	5.147
103×102	5.134

Note: $K = 3, A = 22.5, Ra^* = 2 \times 10^7$

where ϕ was the general variable being tested and $\in$ was a prespecified constant, usually set at 10^{-5}. The agreement between the energy input at the inner cylinder and the energy output at the outer cylinder was also used to check the convergency of the iteration process. The deviation between the input and output energy was usually less than 1.0 per cent.

RESULTS AND DISCUSSION

The presentation will start with the numerical solution for the case of $A = 22.5$, $K = 3$ and $10^3 \leq Ra^* \leq 1.7 \times 10^7$. Isotherms, streamlines and the local and average Nusselt numbers will be presented. Emphasis will be focused on the comparison between the numerical results and the relevant test data, and the comparison between numerical solutions with and without considering the surface radiation. Then, the effect of the aspect ratio on the overall heat transfer result will be discussed. Finally, the numerical results obtained from the computation considering the imperfection in top and bottom insulation will be briefly introduced.

Temperature and local Nusselt number distributions on the outer surface of the inner cylinder

The local temperature values and the local Nusselt numbers along the outer surface of inner cylinder ($r = r_i + w$) are plotted as a function of Rayleigh numbers for the cases with and without considering radiation in *Figures 3* and *4*, respectively. For the simplicity of later writing, the outer surface of the inner cylinder will simply be called inner wall hereafter. A typical temperature profile along the inner wall for $Ra^* = 1.17 \times 10^5$ obtained experimentally by Shang *et al.*[4] is also shown in *Figure 3*. As can be seen there, at low Rayleigh number, such as $Ra^* = 1.02 \times 10^4$, the difference between the two temperature profiles is rather small, indicating that the effect of radiation on the inner wall temperature at low Rayleigh numbers is not appreciable. As the Rayleigh number is increased up to $Ra^* \approx 10^5$ and further, the effect of radiation becomes

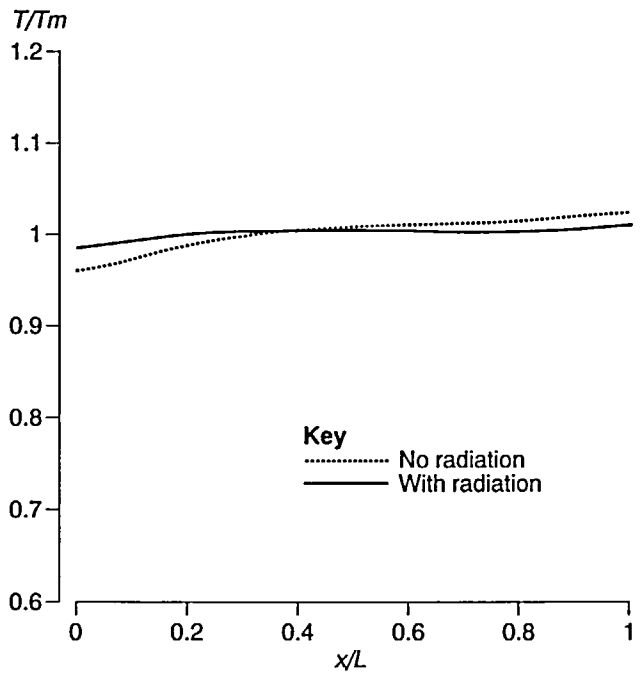

Figure 3a Temperature profiles on inner wall ($Ra^* = 1.02 \times 10^4$)

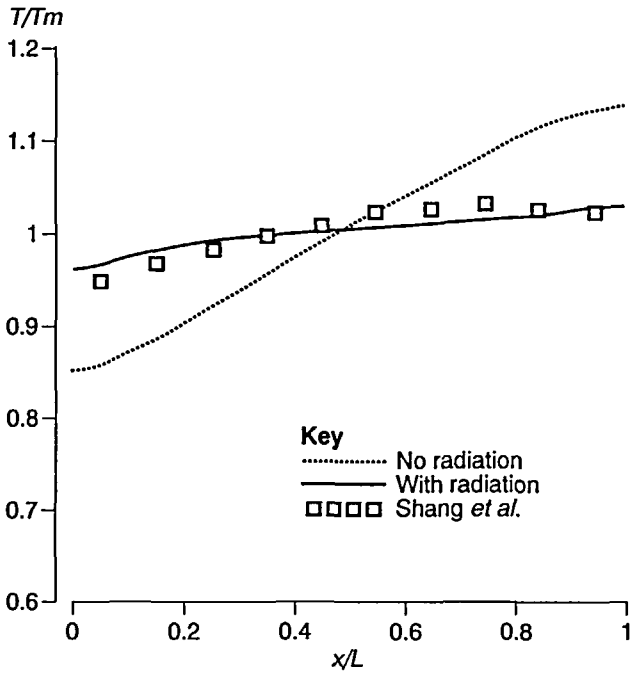

Figure 3b Temperature profiles on inner wall ($Ra^* = 1.17 \times 10^5$)

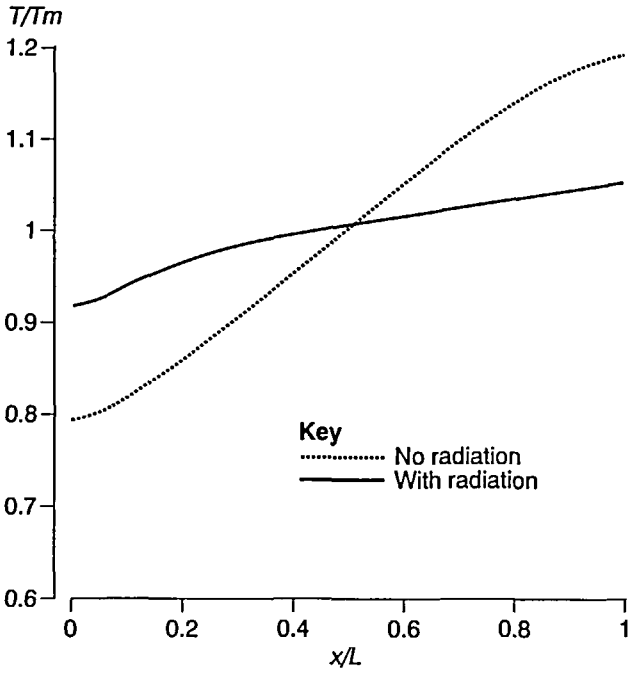

Figure 3c Temperature profiles on inner wall ($Ra^* = 1.04 \times 10^6$)

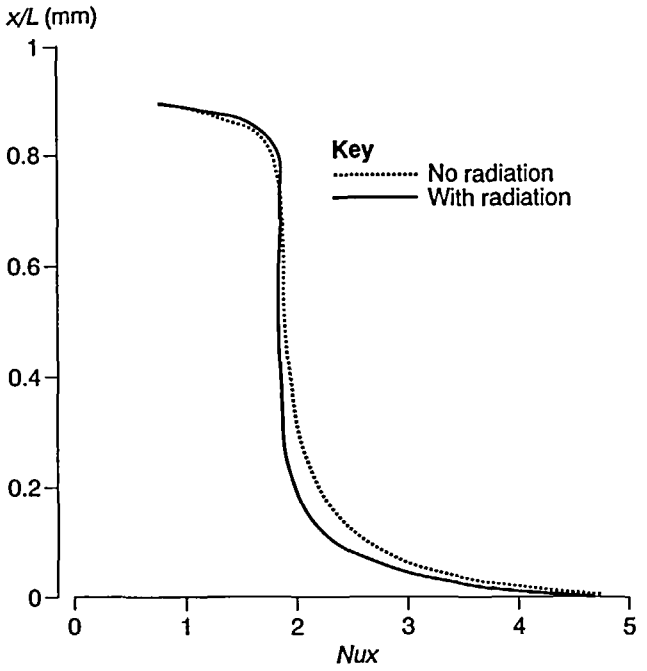

Figure 4a Local Nusselt number distribution on inner wall ($Ra^* = 1.02 \times 10^4$)

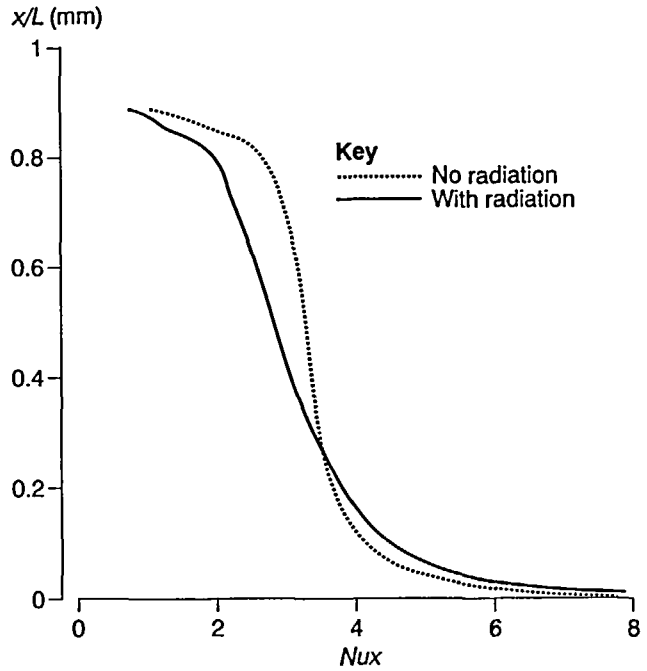

Figure 4b Local Nusselt number distribution on inner wall ($Ra^* = 1.17 \times 10^5$)

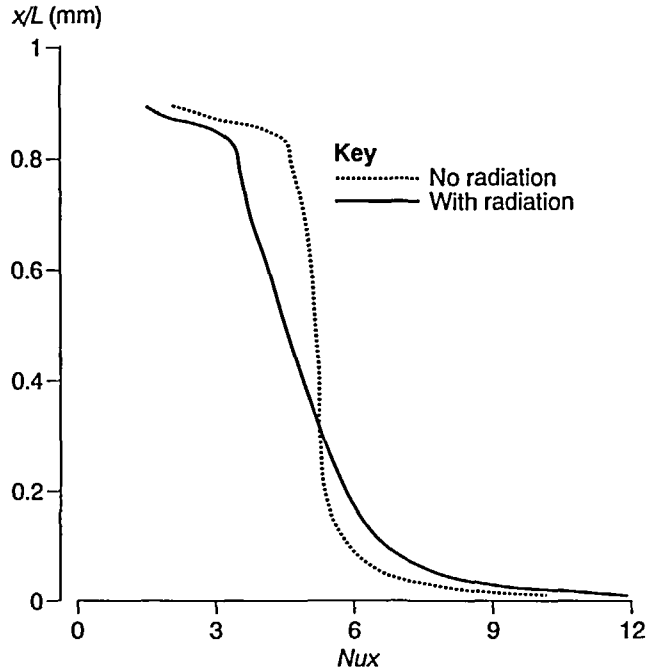

Figure 4c Local Nusselt number distribution on inner wall ($Ra^* = 1.04 \times 10^6$)

appreciable. The wall temperature distribution for the case with radiation considered is greatly evened compared with that without radiation considered. The temperature profile without radiation considered varies strongly with the distance from the bottom. The numerical results with radiation considered for $Ra^* = 1.17 \times 10^5$ agrees well with the experimental profile obtained by Shang *et al.*[4] This reveals that thermal radiation has a role of flattening the temperature profile on the inner wall.

Similar to the situation of temperature profile, the effect of radiation on the local Nusselt number distribution on the inner wall at a low Rayleigh number is not appreciable, while it becomes significant at higher Rayleigh numbers. The consideration of thermal radiation makes the local Nusselt number decrease at the upper part of the inner wall and increase at its lower part compared with the case without consideration of radiation. In other words, thermal radiation has a function of evening the natural convection heat transfer rate in the middle part of the vertical inner wall. This is consistent with the variation in the inner wall temperature distribution shown in *Figure 3*.

Thus it can be concluded that for the thermal boundary conditions studied in this paper, the surface thermal radiation of the inner wall should be taken into account. Therefore, in the discussion of contour maps of streamlines and isotherms, only the results with surface radiation considering will be presented.

Isotherms and streamlines

Isotherms and streamlines for the cases of $K = 3$ and $A = 22.5$ with surface radiation considered are shown in *Figure 5* for $Ra^* = 1.02 \times 10^4$, 1.17×10^5 and 1.04×10^6. As can be seen there, at $Ra^* = 1.02 \times 10^4$, the fluid motion takes the form of a single cell. The centre of the recirculating flow is almost in the middle of the annulus. The isotherms are a group of vertical straight lines except at the two ends. This indicates that the heat transfer is dominated by conduction, in spite of the occurrence of convection in this case.

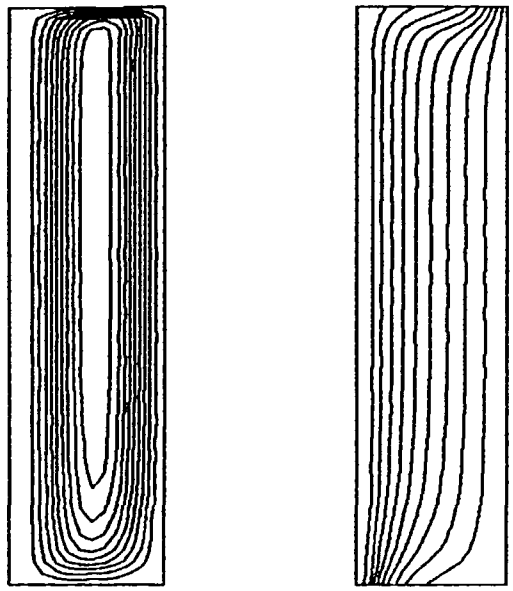

Figure 5a Streamlines and isotherms with radiation ($Ra^* = 1.02 \times 10^4$)

As the Rayleigh number is increased (for example, up to 1.17×10^5), the convective effects become more pronounced. The centre of the circulating flow moves towards the top wall and the isotherms start to cluster near the inner wall. As the Rayleigh number increases to 10^6, a secondary

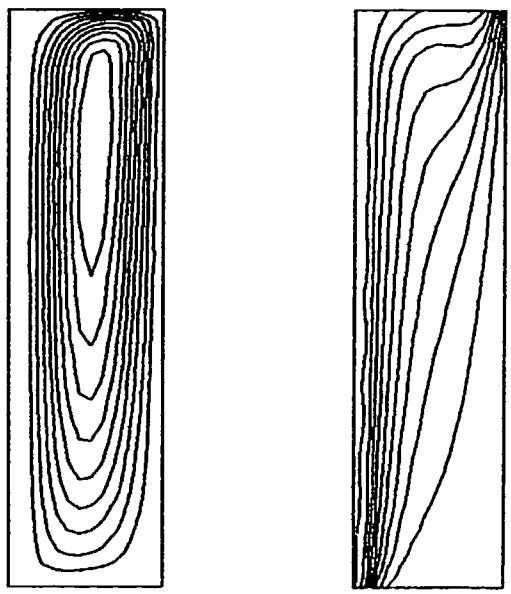

Figure 5b Streamlines and isotherms with radiation ($Ra^* = 1.17 \times 10^5$)

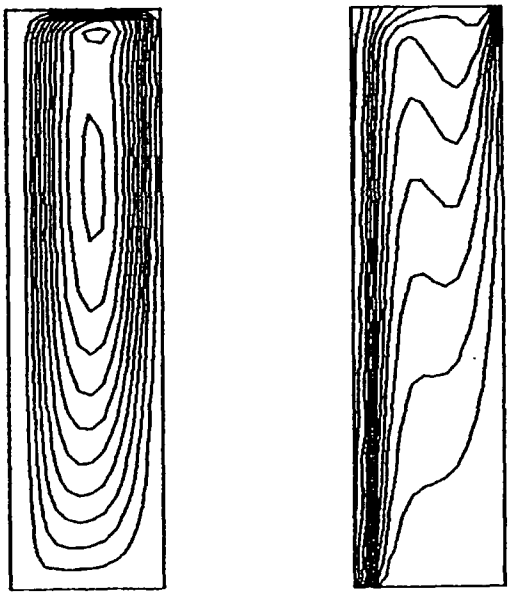

Figure 5c Streamlines and isotherms with radiation ($Ra^* = 1.04 \times 10^6$)

flow appears at the top zone of the annulus, a severe temperature reverse takes place, and the flow near the inner wall exhibits some character of boundary layer type, characterized by a larger temperature gradient normal to the wall. In this case, the heat transfer is dominated by convection.

Overall heat transfer results

For the presentation of the overall heat transfer results, two parameters may be used, i.e. the average Nusselt number, Nu, and the equivalent relative thermal conductivity, K_{eq}, which is defined as

$$K_{eq} = \frac{q_i r_i \ln K}{\Delta T}$$

where ΔT is the average temperature difference between inner and outer wall of the enclosure.

The values of Nu and K_{eq} are related by the following equation:

$$Nu = \frac{K_{eq}(K-1)}{\ln K}$$

where the gap width ($\delta = r_o - r_i - w$) is adopted as the characteristic length in Nu. For comparison purposes, K_{eq} will be used to present the numerical results.

In the comparison of the overall heat transfer character obtained from numerical solutions with and without considering surface heat transfer, one must pay attention to following subtle difference between the two solutions. For the solutions without considering surface radiation, the total heat input, q, at the inner surface of the inner cylinder is fully transferred by the natural convection in the enclosure, while for the solutions with considering the surface radiation, a minor part of the input heat flux q is transferred from the inner wall to the outer wall by radiation. Let the average heat flux of radiation be q_r, then the convective heat transfer rate is only $(q - q_r)$. Since it is the convective heat transfer rate and the related correlation that we are now searching for, the

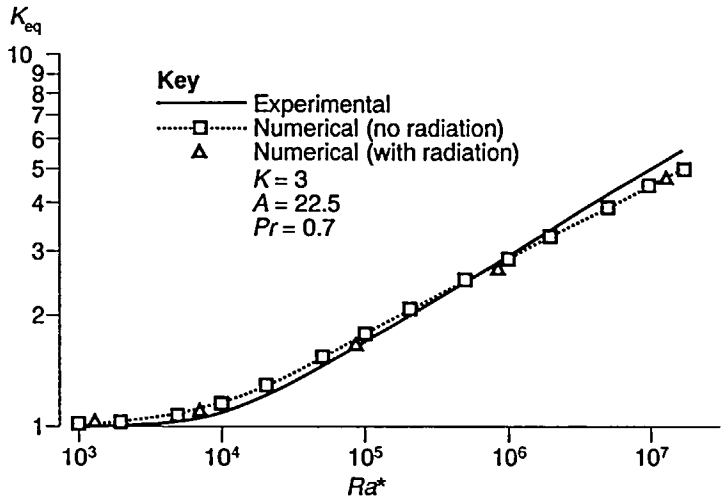

Figure 6 Comparison of numerical and experimental heat transfer results

value of $(q - q_r)$ should be used to determine the related Rayleigh number Ra^* for the solution considering radiation. In *Figure 6*, the results of the two numerical solutions are presented in terms of K_{eq} versus Ra^*. It can be seen that when the above-mentioned subtle difference in Ra^* of the two solutions is taken into account, the overall heat transfer character of the two situations behaves almost identically. This implies that, although the surface radiation have a rather significant effect on the distributions of the inner wall temperature and the local Nusselt number, the overall heat transfer character by natural convection is not affected for the cases studied.

In *Figure 6*, a solid line is drawn which represents the empirical correlation obtained by Shang *et al.*[4] It should be noted that in their experiments, a technique quite similar to that of Sheriff[1] was adopted to subtract the radiation and conduction heat transfer from the total power input, i.e. the heat flux in the definition of Ra^* is purely transferred by natural convection. This is consistent with the above-mentioned data reduction method. It can be seen that the agreement between the experimental and numerical results is quite good, with a maximum deviation of 11 per cent accuracy at $Ra^* = 1.7 \times 10^7$.

Dependence of K_{eq} *on* A

The heat transfer results have also been obtained numerically for the combinations of radius ratio and aspect ratio, $K = 3, A = 10, 15, 20, 25, 30$, as shown in *Figure 7*. As can be seen in the figure, the average relative conductivity increases with Ra^* for all aspect ratios investigated, while the dependence of K_{eq} on A is not all the same for the Rayleigh numbers investigated. At low Rayleigh number($Ra^* \approx 10^4$), the dependence of K_{eq} on A is very weak. This is because, in the low Rayleigh number region, the dominating heat transfer mechanism is the radial heat conduction, which is not dependent on the length of the cylinder. While at high Rayleigh numbers, the effect of A on K_{eq} becomes appreciable and K_{eq} decreases with the increase in A. Thus, the dependence of K_{eq} on A also depends on Rayleigh numbers. This result seems not to support the usual practice adopted in the literature where the dependence of K_{eq} or average Nusselt number on A was incorporated by a constant exponent in A term for the whole Ra^* range investigated.

Effect of insulation imperfection on the inner wall temperature distribution

As mentioned above, to investigate the imperfection in insulation the computation domain was extended to the region confined by the dashed line shown in *Figure 1*. The numerical results of

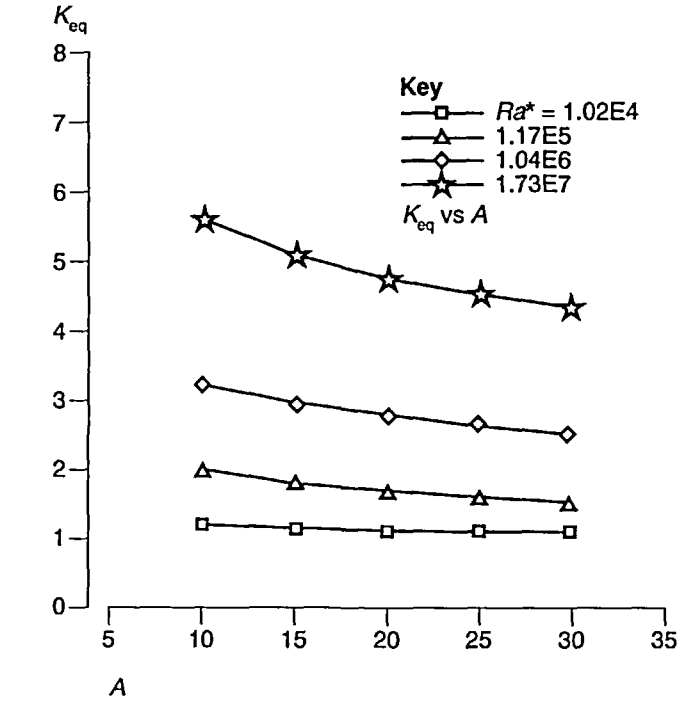

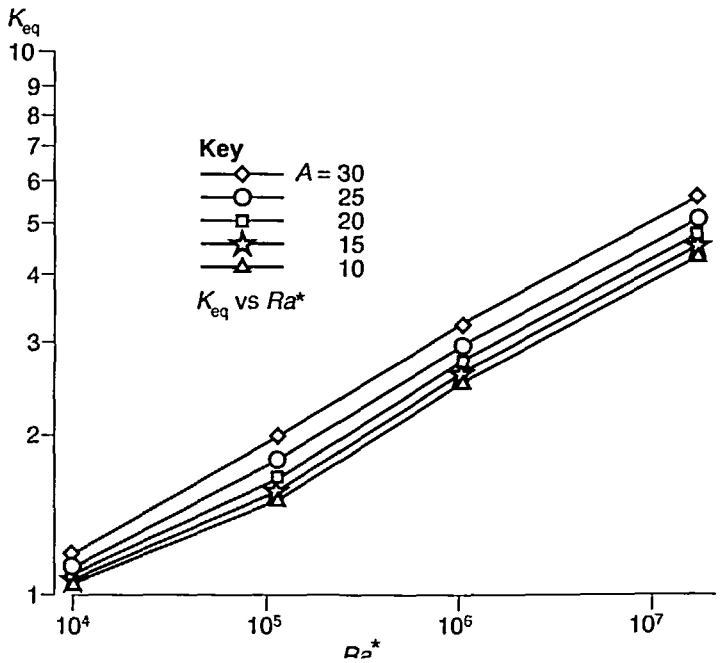

Figure 7 Variation of K_{eq} with aspect ratio and Rayleigh number ($K = 3$)

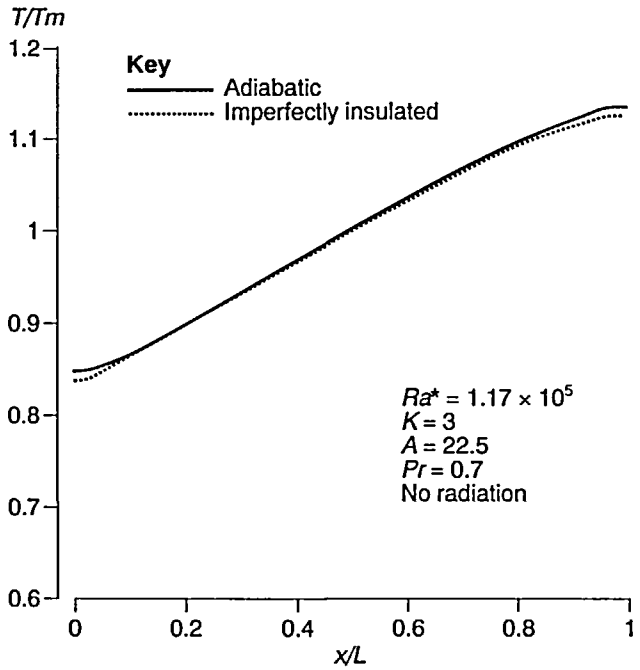

Figure 8 Effect of imperfection in insulation on inner wall temperature distribution

inner wall temperature distribution are presented in *Figure 8*, where the results obtained for the perfect insulation are also presented for comparison purposes. Both computations were conducted without considering surface radiation. It can be seen that, for the two situations compared, the imperfection in top-and-bottom insulation only has a very weak effect on the inner wall temperature distribution. In addition, from a practical point of view, the insulation technique used in Shang's[4] experiment may be considered perfect enough to neglect the end loss through heat conduction. Therefore, all the computational results presented above were obtained with adiabatic boundary conditions at top and bottom surfaces.

CONCLUSIONS

Numerical analysis has been conducted for natural convection of air in a vertical annulus with the inner surface of the inner cylinder maintained at constant heat flux. The outer cylinder is maintained at constant temperature and the top and bottom plates are assumed to be insulated. The effect of the inner wall radiation has been examined in detail. The parameter range investigated is $K = 3$, $10 \leq A \leq 30$, and $10^3 \leq Ra^* \leq 1.7 \times 10^7$. The following conclusions can be drawn:

(1) The effect of radiation on temperature profile and local Nusselt number on the inner wall is significant in a high Rayleigh number region. The surface radiation effect tends to flatten the local temperature and Nusselt number on the major part of the inner wall. The temperature profile calculated for the case with considering radiation is in very good agreement with the measured profile in the literature.

(2) The agreement between the numerical heat transfer results and the experimental results is quite satisfactory, with the maximum difference of less than 11 per cent. In the Rayleigh number range studied, the incorporation of surface radiation on the inner wall does not have an appreciable effect on the overall convective heat transfer character.

(3) The effect of aspect ratio on the average relative conductivity depends on the Rayleigh number, and gradually becomes significant with the increase in Rayleigh numbers.

ACKNOWLEDGEMENT

This work was supported by National Natural Science Foundation of China.

REFERENCES

1 Sheriff, N., Experimental investigation of natural convection in single and multiple vertical annuli with high pressure carbon dioxide, *Proceedings of 3rd International Heat Transfer Conference*, Chicago, IL, **2**, 132-138 (1966)
2 Keyhani, M., Kulacki, F.A. and Chrisensen, R.N., Free convection in a vertical annulus with constant heat flux on the inner wall, *ASME Journal of Heat Transfer*, **105**, 454-459 (1983)
3 Bhushan, R., Keyhani, M., Christensen, R.N. and Kulacki, F.A., Correlation equations for free convection in a vertical annulus with constant heat flux on the inner wall, *ASME Journal of Heat Transfer*, **105**, 910-912 (1983)
4 Shang, H.M., Wu, Q.J. and Tao, W.Q., Experimental and numerical investigations of natural convection in vertical annuli, *Journal of XI'an Jiaotong University*, **23**, 1, 9-20 (1989)
5 Khan, J.A. and Kumar, R., Natural convection in vertical annuli: a numerical study for constant heat flux on the inner wall, *ASME Journal of Heat Transfer*, **111**, 909-915 (1989)
6 Sparrow, E.M. and Cess, R.D., *Radiation Heat Transfer*, Augmented Ed., McGraw-Hill, NY (1978)
7 Tao, W.Q., *Numerical Heat Transfer*, Xi'an Jiaotong University Press, Xi 'an, China (1988)
8 Yang, M., Wang, Y.Q., Fu, Y.H. and Tao, W.Q., A numerical method for coupled conduction and convection heat transfer with surface radiation, *Journal of Xi'an Jiaotong University*, **26**, 6, 25-31 (1992)
9 Zhao, C.Y. and Tao, W.Q., Natural convection in conjugated single and double enclosures, *Wärme-und Stoffübertragung*, **30**, 175-182 (1995)